Cancer Biology and Signal Transduction

Molecular Cancer Therapeutics

MiR-134/487b/655 Cluster Regulates TGF-β–Induced Epithelial–Mesenchymal Transition and Drug Resistance to Gefitinib by Targeting *MAGI2* in Lung Adenocarcinoma Cells

Kazuhiro Kitamura, Masahiro Seike, Tetsuya Okano, Kuniko Matsuda, Akihiko Miyanaga, Hideaki Mizutani, Rintaro Noro, Yuji Minegishi, Kaoru Kubota, and Akihiko Gemma

Abstract

Epithelial–mesenchymal transition (EMT) has recently been recognized as a key element of cell invasion, migration, metastasis, and drug resistance in several types of cancer, including non–small cell lung cancer (NSCLC). Our aim was to clarify microRNA (miRNA)-related mechanisms underlying EMT followed by acquired resistance to epidermal growth factor receptor tyrosine kinase inhibitor (EGFR-TKI) in NSCLC. miRNA expression profiles were examined before and after transforming growth factor β1 (TGF-β1) exposure in four human adenocarcinoma cell lines with or without EMT. Correlation between expressions of EMT-related miRNAs and resistance to EGFR-TKI gefitinib was evaluated. miRNA array and real-time quantitative reverse transcription PCR (qRT-PCR) revealed that TGF-β1 significantly induced overexpression of miR-134, miR-487b, and miR-655, which belong to the same cluster located on chromosome 14q32, in lung adenocarcinoma cells with EMT. *MAGI2* (membrane-associated guanylate kinase, WW, and PDZ domain–containing protein 2), a predicted target of these miRNAs and a scaffold protein required for PTEN, was diminished in A549 cells with EMT after the TGF-β1 stimulation. Overexpression of miR-134 and miR-487b promoted the EMT phenomenon and affected the drug resistance to gefitinib, whereas knockdown of these miRNAs inhibited the EMT process and reversed TGF-β1–induced resistance to gefitinib. Our study demonstrated that the miR-134/487b/655 cluster contributed to the TGF-β1–induced EMT phenomenon and affected the resistance to gefitinib by directly targeting *MAGI2*, in which suppression subsequently caused loss of PTEN stability in lung cancer cells. The miR-134/miR-487b/miR-655 cluster may be a new therapeutic target in patients with advanced lung adenocarcinoma, depending on the EMT phenomenon. *Mol Cancer Ther; 13(2); 444–53. ©2013 AACR.*

Introduction

Lung cancer was reported to be the leading cause of cancer-related death worldwide in males, and the second leading cause in females (1). Molecular-targeted therapies have been developed recently for non–small cell lung cancer (NSCLC). Thus, patients with NSCLC with epidermal growth factor receptor (EGFR) gene mutations have shown a dramatic response to EGFR tyrosine kinase inhibitors (EGFR-TKI) such as gefitinib and erlotinib (2, 3). Our group and others have recently reported that first-line gefitinib treatment in patients with advanced NSCLC with EGFR mutations improved progression-free survival in randomized phase III studies (4–6). Therefore, gefitinib has been recognized as a first-line treatment of patients with NSCLC with EGFR activating mutations. These results represent a milestone toward personalized medicine in NSCLC oncology. Despite the advances in chemotherapy and molecular-targeted therapy, the prognosis of patient with advanced NSCLC is still poor because of metastasis and drug resistance.

Epithelial–mesenchymal transition (EMT), especially that induced by transforming growth factor β1 (TGF-β1), is a progressive biological phenomenon that includes loss of epithelial cell adhesion and induction of a mesenchymal phenotype (7). Previous studies demonstrated that EMT was involved in cell invasion, migration, and metastasis in several types of cancer, including NSCLC (8, 9). Several studies have demonstrated that EMT was associated with reduction of drug sensitivity and acquisition of resistance to EGFR-TKIs in NSCLC, whereas retention of an epithelial phenotype ensured a good response to EGFR-TKIs even in patients with tumors

Authors' Affiliation: Department of Pulmonary Medicine and Oncology, Graduate School of Medicine, Nippon Medical School, Tokyo, Japan

Note: Supplementary data for this article are available at Molecular Cancer Therapeutics Online (http://mct.aacrjournals.org/).

Corresponding Author: Masahiro Seike, Nippon Medical School, 1-1-5, Sendagi, Bunkyo-ku, Tokyo 113-8603, Japan. Phone: 81-3-3822-2131; Fax: 81-3-5685-3075; E-mail: mseike@nms.ac.jp

doi: 10.1158/1535-7163.MCT-13-0448

harboring wild-type *EGFR* genes (10–12). These reports suggested that EMT might be a mechanism of resistance to EGFR-TKI regardless of *EGFR* status.

MicroRNAs (miRNA) are single-strand 18–24nt noncoding molecules that post-transcriptionally modulate gene expression through binding to 3′ untranslated regions (UTR) of target mRNAs (13). miRNAs, which usually induce gene silencing, can function as either tumor suppressors or oncogenes (14). Recent studies revealed that miRNAs were diagnostic, prognostic, and therapeutic biomarkers in lung cancer (15, 16). Our previous study demonstrated that inhibition of miR-21 expression could be used as a therapeutic strategy in connection with EGFR-TKI treatment (17). Several miRNAs have been also identified as regulators of EMT in cancer. EMT was suppressed by miR-200 family members, targeting the transcriptional activators of EMT, ZEB1, and ZEB2 in lung cancer (18, 19). Despite previous reports of miRNAs associated with EMT and cancer, miRNAs and their target genes involved in TGF-β1–induced EMT, resulting in resistance to EGFR-TKIs, are still not fully understood.

In this study, we analyzed miRNA changes to clarify which miRNA was associated with TGF-β–induced EMT followed by acquired resistance to EGFR-TKI. We used four lung adenocarcinoma cell lines with or without the TGF-β–induced EMT phenomenon and demonstrated that the miR-134/487b/655 cluster was associated with TGF-β–induced EMT and played a critical role in EMT through the targeting of membrane-associated guanylate kinase, WW, and PDZ domain–containing protein 2 (*MAGI2*).

Materials and Methods

Cell culture

Eight lung adenocarcinoma cell lines, A549, LC2/ad, PC3, PC9, RERF-LCKJ, RERF-LCMS, PC14, and ABC-1, were used in this study. A549, LC2/ad, and RERF-LCKJ were obtained from the RIKEN Cell Bank; PC3, PC9, and PC14 were obtained from Immuno-Biological laboratories; and RERF-LCMS and ABC-1 were obtained from the Health Science Research Resources Bank. These cell lines have been obtained from 2003 to 2011, were amplified and frozen, and one aliquot of each was thawed for this project, although no authentication was done by the authors. All cells were routinely screened for the absence of mycoplasma. These cell lines were maintained in RPMI 1640 medium (GIBCO) supplemented with 10% fetal bovine serum (FBS).

RNA extraction and microarray analysis

Total RNA was extracted from the four lines with TRIzol reagent (Invitrogen) as described previously (20, 21). Concisely, 5 μg of total RNA was used for hybridization on miRNA microarray chips containing 667 probes with the TaqMan Array Human MicroRNA A + B Cards Set v2.0 (Life Technologies) on a 7900 Real Time PCR System (Applied Biosystems). Processed slides were scanned with a PerkinElmer ScanArray XL5K Scanner. Experimental data were analyzed by DataAssist Software (Life Technologies) using RNU44 and RNU48 as endogenous controls. Ct values were provided from all miRNAs represented on the cards and fold changes in expression were calculated using the $\Delta\Delta C_t$ method. Expression levels of MammU6 on the array card were defined as positive controls for the purpose of ddCt calculation. The microarray data have been deposited in NCBIs Gene Expression Omnibus (GEO; http://www.ncbi.nlm.nih.gov/geo/) and are accessible through GEO Series accession number GSE51828 (release date October 30, 2013).

Real-time quantitative reverse transcription PCR

The MAGI2 mRNA expression and miR-134/478b/655 levels were measured by real-time quantitative reverse transcription PCR (qRT-PCR) using TaqMan Gene Expression Assay and TaqMan MicroRNA Assay (Applied Biosystems), respectively. GAPDH (glyceraldehyde-3-phosphate dehydrogenase) or RNU66 was determined as an internal control (Applied Biosystems). miRNA and MAGI2 mRNA expressions were quantified and reported by the relative standard curve method.

Antibodies and Western blot analysis

Cells were dissolved in buffer containing 50 mmol/L Tris-HCl, pH 7.6, 150 mmol/L NaCl, 0.1% sodium dodecyl sulfate, 1% Nonidet *P*-40, and 0.5% sodium-deoxycholate. The lysates were cooled in ice for 30 minutes, and then centrifuged at 13,000× *g* for 30 minutes. Each protein (10 μg) of the collected supernatant was separated by SDS-PAGE on 12% gels and then transferred to a nitrocellulose membrane. The membrane, after a block with 5% skimmed milk, was incubated with antibodies to E-cadherin, N-cadherin, vimentin, β-actin, PTEN, p-PTEN (Ser 380; Cell Signaling Technology), and MAGI2 (AIP1; Abcam Biochemicals). Each protein was detected by immunoblotting with ECL-Plus reagents (GE Healthcare Bio-Science Corp).

Oligonucleotide transfection

TGF-β1 was purchased from R&D system. Cells were exposed to 5 ng/mL TGF-β for the indicated time. siRNA targeting MAGI2 and negative control were purchased from Ambion and Invitrogen, respectively. miR-134 and miR-487b precursors (pre-miR-134 and pre-miR-487b), their negative control (pre-NC), miR-134 and miR-487b inhibitors (anti-miR-134/487b) and their cognate negative control (anti-NC) were synthesized by Ambion. All precursors and inhibitors were treated with lipofectamin 2000 transfection reagent 24 hours after seeding, according to the manufacturer's instructions (Life Technologies). The precursor and inhibitor complexes were transfected into cells at a final concentration of 40 nmol/L. The final concentration of miRNA was determined according to the recommend dose of lipofectamin 2000 transfection

protocol (Invitrogen). The transfection medium was replaced 6 hours later. After the transfection at 24 hours, 5 ng/mL TGF-β1 was added to the medium, which was then incubated at 37°C for 48 hours.

Growth-inhibition assay

Gefitinib was purchased from Seleck Chemicals. A549 cells (5,000 cells/well) were seeded into 96-well plates for 24 hours. The cells were incubated in the various concentrations of gefitinib for 72 hours at 37°C after exposure to pre-miR-134, pre-miR-487b, or pre-miR-ctl at a final concentration of 40 nmol/L for 24 hours. Likewise, the cells with both anti-miR-134 and anti-miR-487b, or anti-miR-ctl were exposed to 5 ng/mL TGF-β1 for 48 hours, and then received the gefitinib treatment. After the incubation in various concentrations of gefitinib, each well was transfected with 20 μL of MTT solution (5 mg/mL in PBS), then continuously maintained for a further 4 hours at 37°C as previously described (22, 23). Finally, the absorbance was measured using a microplate reader with a test wavelength of 560 nm.

Luciferase assay

Luciferase reporter constructs containing portions of the MAGI2 3′UTRs were generated by GeneCopoeia, Inc.. A549 cells were cultured in 24-well plates for 24 hours and cotransfected with 800 ng/uL of MAGI2 3′UTR reporter constructs and 50 nmol/L of pre-miR-134 or pre-miR-487b, or pre-NC using lipofectamine 2000 for 24 hours. After transfection, cells were harvested, lysed, and assayed with the Dual-Luciferase Reporter Assay Kit (Promega) according to the manufacturer's instructions. Firefly luciferase activity was normalized to renilla luciferase activity for each transfected well. Each experiment was performed in duplicate and repeated three times.

Statistical analysis

Statistical analysis was performed using SigmaPlot software (version 12.0; Systat Software, Inc.). Data were expressed as a mean (SD) of three independent experiments and evaluated with the Student *t* test.

Result

miRNA expression profiles of lung adenocarcinoma cells with TGF-β1–induced EMT

Four lung adenocarcinoma cell lines, A549, LC/ad2, PC3, and PC9, were stimulated by TGF-β1. Figure 1A shows the conversion from epithelial cells to mesenchymal cells, characterized by spindle-type cell morphology in A549 and LC2/ad cells. On the other hand, PC3 and PC9 cells did not show this morphological change (Fig. 1B). We evaluated the expression levels of EMT markers in A549 and LC2/ad cells treated with TGF-β1 to confirm the EMT phenomenon. A549 and LC2/ad cells after TGF-β1 stimulation displayed reduced epithelial

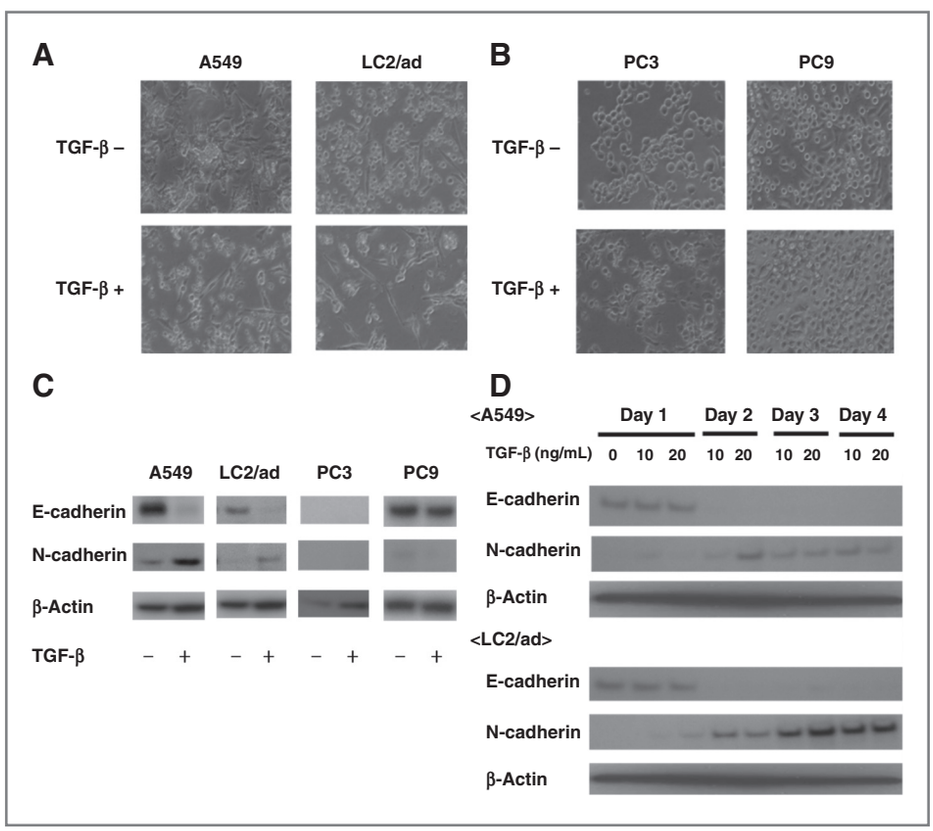

Figure 1. Four lung adenocarcinoma cell lines were divided into EMT-positive and EMT-negative groups based on characteristic differences in cell morphology and in protein expression of epithelial or mesenchymal markers after TGF-β1 stimulation. A and B, four cell lines were treated with 5 ng/mL of TGF-β1 for 72 hours. The change in morphology was observed under a light microscope. A549 or LC2/ad cells treated with TGF-β1 showed mesenchymal features after the TGF-β1 treatment. In contrast, PC3 or PC9 cells still showed epithelial features after the TGF-β1 treatment. C, E-cadherin and N-cadherin expressions in the four cell types after the TGF-β1 stimulation were evaluated by Western blot analysis. D, E-cadherin and N-cadherin expression levels of A549 and LC2/ad cells treated with 10 or 20 ng/mL TGF-β1 were evaluated at 24, 48, and 72 hours. E-cadherin downregulation and N-cadherin upregulation depended on concentration and time of TGF-β1 exposure.

marker E-cadherin and increased mesenchymal cell marker N-cadherin expressions, when compared with PC3 and PC9 cells without TGF-β1 exposure (Fig. 1C). The time courses of decreased expression of E-cadherin and increased expression of N-cadherin, through TGF-β1 transfection, were observed in A549 and LC2/ad cells (Fig. 1D). A549 and LC2/ad cells were therefore recognized as lung cancer cells with the TGF-β1–induced EMT phenomenon. Next, we evaluated miRNA expression profiles in EMT-positive lines (A549 and LC2/ad) and EMT-negative lines (PC3 and PC9) before and after exposure to TGF-β1 using microRNA arrays. After the TGF-β1 treatments, the expression levels of 11 miRNAs in EMT-positive cells were increased significantly more than the expression levels in EMT-negative cell (Fig. 2A). The miRBase database (http://www.mirbase.org) indicated that among the 11 miRNAs, miR-134, miR-487b, and miR-655 belonged to the same miRNA cluster on chromosome 14q32. The expression of these three miRNAs before and after exposure to TGF-β1 was validated by qRT-PCR (Fig. 2B–D). In contrast, the expression levels of these three miRNA in EMT-negative cells were unaffected by exposure to TGF-β1 (Fig. 2B–D). Moreover, we evaluated miR-134/478b/655 expression levels in eight lung adenocarcinoma cells without TGF-β1 stimulation, previously performed by the TaqMan MicroRNA Array (24). Previous reports demonstrated that RERF-LC-KJ and RERF-LC-MS were recognized as EMT-positive cells (25, 26). Four EMT-positive cells exhibited higher expression levels of three miRNAs than did those of four EMT-negative cells (Supplementary Fig. S1). Thus, we have identified miR-134, miR-487b, and miR-655 as candidate miRNAs associated with the EMT phenomenon in lung cancer.

miR-134 and -487b regulated TGF-β1–induced EMT in A549 cells

We further examined whether miR-134 and miR-487b regulated TGF-β1–induced EMT. Unfortunately, the role of miR-655 on TGF-β1–induced EMT could not be evaluated because the specific miR-655 precursor or inhibitor was commercially unavailable. We confirmed that mature miR-134/487b of A549 cells were significantly increased by miR-134 or miR-487b precursors (pre-miR-134 or pre-miR-487b) and decreased by miR-134 or miR-487b inhibitors (anti-miR-134 and anti-miR-487b; Supplementary Fig. S2A and S2B). First, A549 cells were transfected with pre-miR-134 or pre-miR-487b and control precursor

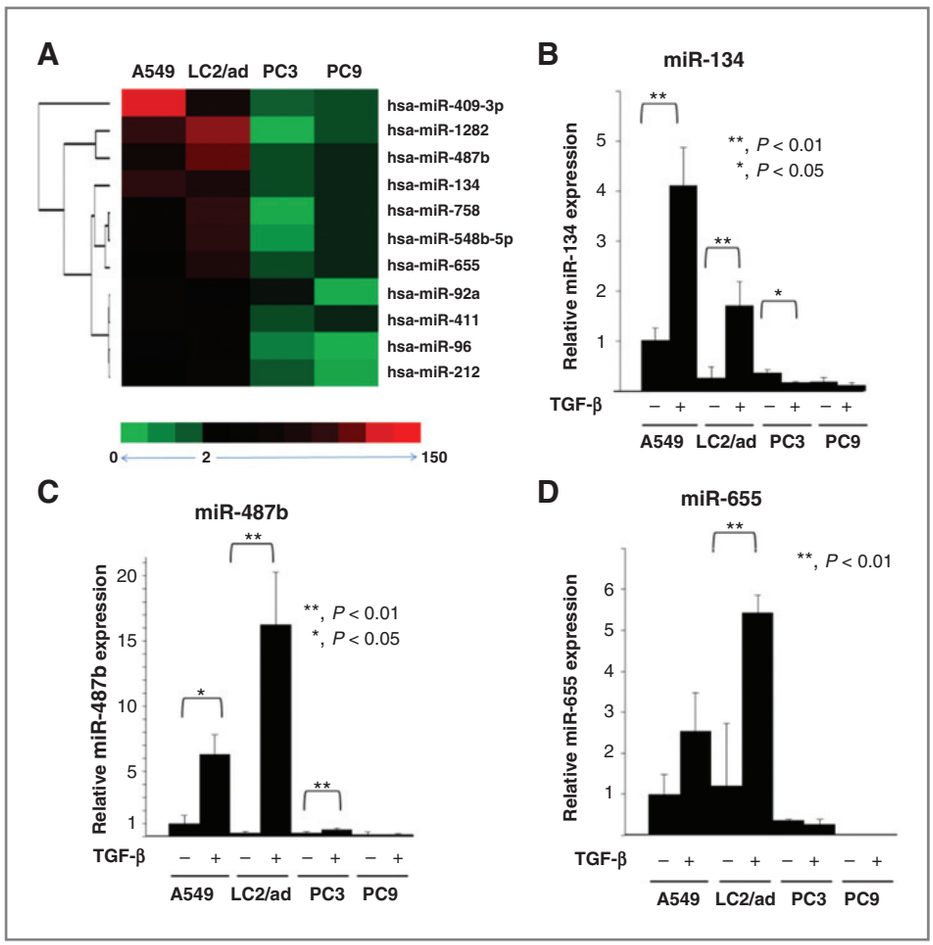

Figure 2. Differences in miRNA expression between EMT-positive and EMT-negative cells before and after TGF-β1 exposure. A, miRNA expression profiles before and after TGF-β1 exposure were assessed in the four cell types by TaqMan miRNA arrays. Relative ratios of miRNAs in cells after TGF-β1 exposure were calculated when compared with the cells before TGF-β1 exposure. Eleven miRNAs were detected as EMT-associated miRNAs. B to D, expression of three miRNAs in four lung cancer cell lines was confirmed by qRT-PCR analysis. In the EMT-positive A549 and LC2/ad cells, expression of miR-134, miR-487b, and miR-655 was significantly upregulated after TGF-β1 treatment.

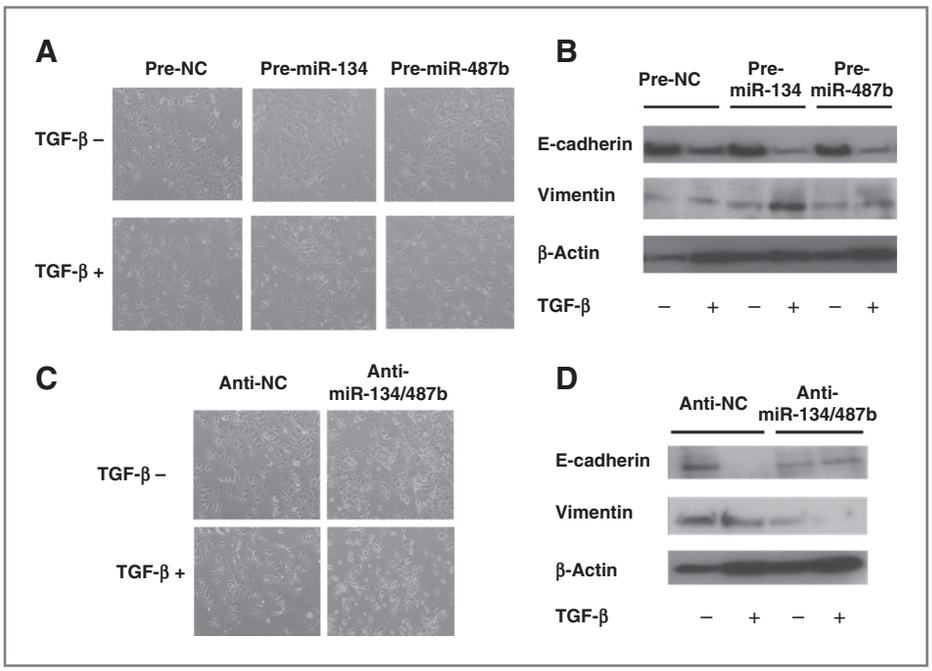

Figure 3. TGF-β1–induced EMT was promoted by miR-134 and miR-487b in A549 cells. A, A549 cells treated with pre-miR-134 or pre-miR-478b together with 5 ng/mL of TGF-β1 seemed to have more spindle morphology under a light microscope. B, E-cadherin and vimentin expression by Western blot analysis. Low expression of E-cadherin and high vimentin expression were shown in A549 cells treated with pre-miR-134 or pre-miR-487b together with TGF-β1. C, morphologic change induced by the TGF-β1 exposure was recovered in A549 cells treated with anti-miR-134 plus anti-miR-478b for 48 hours in comparison with the control. D, after TGF-β1 exposure for 24 hours, the expression level of E-cadherin in A549 cells treated with anti-miR-134 plus anti-miR-478b for 48 hours was diminished less than the E-cadherin expression level in A549 cells treated with anti-NC. In addition, anti-miR-134/478b treatment led to inhibition of vimentin expression induced by TGF-β1 exposure.

(pre-NC) and exposed to 5 ng/mL of TGF-β1 for 72 hours. After the TGF-β1 treatment, A549 cells transfected with pre-miR-134 or pre-miR-487b seemed to be more uniformly mesenchymal than A549 cells transfected with pre-NC (Fig. 3A). Western blot analysis showed that A549 cells treated with pre-miR-134 or pre-miR-487b had diminished E-cadherin expression, and that A549 cells treated with pre-miR-134 after the TGF-β1 stimulation had increased expression of vimentin, the mesenchymal cell marker (Fig. 3B). Next, we investigated the effect of inhibition of the two miRNAs on TGF-β1–induced EMT in A549 cells. A549 cells transfected with a combination of anti-miR-134/487b or control inhibitor (anti-NC) were exposed to TGF-β1 for 72 hours. Figure 3C demonstrates that transfection of anti-miR-134/487b inhibited the conversion from epithelial phenotype to mesenchymal phenotype after TGF-β1 stimulation. Western blot analysis also showed that E-cadherin expression was still present after the anti-miR-134/487b treatments, resulting in prevention of TGF-β1–induced EMT in A549 cells (Fig. 3D). These results demonstrated that miR-134 and miR-487b actively contributed to TGF-β1-induced EMT in A549 cells.

TGF-β1 regulated MAGI2 expression through miR-134 and miR-487b

Our results indicated that miR-134 and miR-487b promoted TGF-β1–induced EMT. We next proceeded to identify potential targets using the microRNA.org database (http://www.microrna.org/microrna/home), a comprehensive resource of miRNA target predictions and expression profiles. We found that miR-134, miR-487b, and miR-655 belonged to the same cluster of miRNAs that commonly target *MAGI2*. Furthermore, *MAGI2* could be predicted as a target of miR-134 and miR-655 by another database, Target Scan 5.0–5.2 (http://www.targetscan.org/). Figure 4A shows the regions of 3′UTR of the *MAGI2* gene that could serve as binding sites for the three miRNAs based on the prediction of microRNA.org. To confirm whether TGF-β1 exposure diminished the expression levels of MAGI2 mRNA via upregulating these miRNAs, we evaluated MAGI2 mRNA expression by qRT-PCR in four types of lung cancer cells before and after treatment with TGF-β1. TGF-β1 stimulation decreased MAGI2 expression in the EMT-positive cells, but not in the EMT-negative cells (Fig. 4B). Next, we examined whether overexpression of miR-134 or miR-487b diminished MAGI2. The qRT-PCR and Western blot analyses showed that the pre-miR-134 or pre-miR-487b treatments induced downregulation of both mRNA and protein expression of MAGI2 in A549 cells (Fig. 4C). In contrast, expression levels of MAGI2 mRNA and protein were increased in A549 cells after treatment with anti-miR-134 and anti-miR-487b with or without TGF-β1 exposure (Fig. 4D). We also performed a luciferase reporter assay to

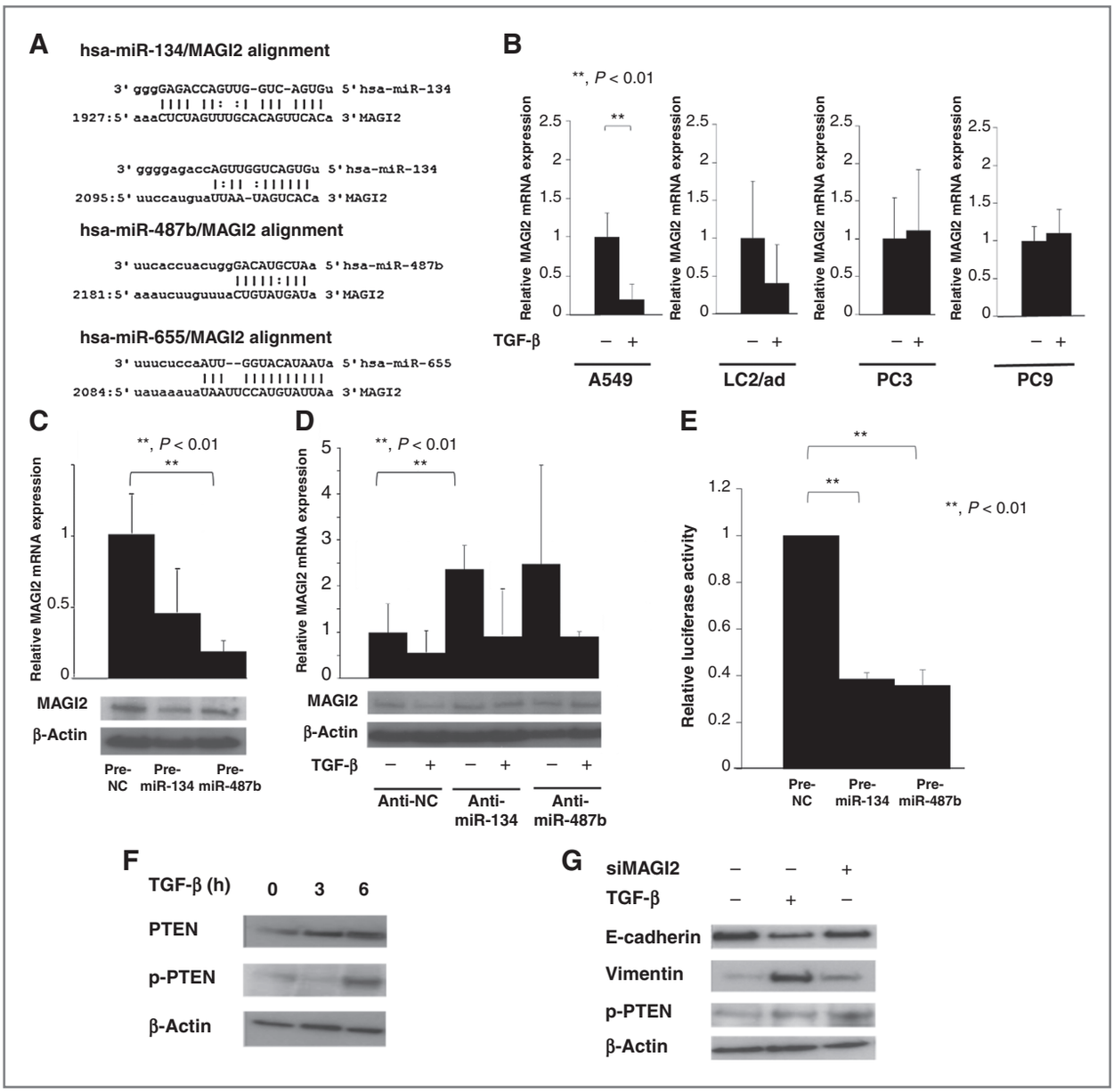

Figure 4. TGF-β1 regulates *MAGI2* expression. A, predicted duplex formations by human MAGI2 3′UTR and miR-134, miR-487b, or miR-655. B, MAGI2 mRNA expression was decreased in A549 and LC2/ad cells after TGF-β1 exposure for 24 hours. C, after transfection with pre-miR-134 or pre-miR-487 in A549 cells for 24 hours, the expression levels of MAGI2 mRNA and protein were reduced according to qRT-PCR analysis and Western blot analysis, respectively. D, anti-miR-134 or anti-miR-487b was transfected into A549 cells for 24 hours with or without TGF-β1 (5 ng/mL) exposure for a further 48 hours. The qRT-PCR analysis revealed that anti-miR-134 or anti-miR-487b induced an increase in MAGI2 mRNA expression in A549 cells without TGF-β exposure, and with TGF-β exposure there was more residual expression of MAGI2 mRNA in A549 cells than after anti-NC exposure. The Western blot analysis also revealed that MAGI2 expression remained after TGF-β stimulation in A549 cells together with anti-miR-134 or anti-miR-487b. E, miR-134/487b suppressed the luciferase activity of the pGL3-MAGI2 3′UTR reporter. A549 cells were cotransfected with pGL3-MAGI2 3′UTR reporter and pre-NC or pre-miR-134, or pre-miR-487b, and dual luciferase assays were carried out 24 hours after transfection. Data, mean ± SD from three independent experiments. **, $P < 0.01$ when compared with the control cells (paired *t* test). F, TGF-β1 mediated PTEN instability by phosphorylating PTEN. A549 cells were treated with 5 ng/mL TGF-β1 for 0, 3, or 6 hours. TGF-β1 enhanced expression levels of p-PTEN in a time-dependent manner. G, MAGI2 mediated PTEN instability by phosphorylating PTEN. Knockdown of MAGI2 by transfecting specific MAGI2 siRNA for 24 hours caused reduction of E-cadherin and a small gain of vimentin and PTEN phosphorylation.

verify that miR-134/487b directly targets *MAGI2*. We found that cotransfection of miR-134 or miR-487b precursor and MAGI2 3′UTR vector significantly decreased the luciferase activity in A549 cells as compared with the control (Fig. 4E). These data showed that *MAGI2* is a direct target of miR-134/487b. MAGI2, a multidomain

scaffolding protein, contains nine potential protein–protein interaction modules and inhibits cell migration and proliferation via PTEN in HCC cells (27). TGF-β1 stimulation or inhibition of MAGI2 was attenuated in A549 cells with PTEN phosphorylation (Fig. 4F and G). PTEN silencing played a critical role in the EMT phenomenon caused by miR-134 and miR-487b–induced MAGI-2 inhibition in A549 cells. These findings suggested that expression of miR-134 and miR-487b consequently played a key role in TGF-β1–induced EMT by targeting *MAGI2*, leading to PTEN inactivation in lung adenocarcinoma cells.

miR-134 and -487b induced drug resistance to gefitinib

Finally, we evaluated whether miR-134 and miR-487b elicited resistance to EGFR-TKI. A549 cells treated with pre-miR-134 or pre-miR-487b as well as TGF-β1 were more resistant to gefitinib than were A549 parent cells (Fig. 5A). We also measured the response to gefitinib in A549 cells after treatment with miR-134 and miR-487b inhibitors in combination with TGF-β1. Anti-miR-134 plus anti-miR-487b transfection restored the resistance to gefitinib caused by TGF-β1 (Fig. 5B). Therefore, miR-134 and miR-487b activated by TGF-β1 could lead to resistance to gefitinib.

Discussion

Identification of mechanisms of drug resistance to EGFR-TKIs and development of methods to overcome resistance are required for improvement of the prognosis of patients with advanced NSCLC. Approximately 50% of patients with EGFR-mutant lung cancer who develop acquired resistance to EGFR-TKI have a second-hit mutation, T790M, in exon 20 (28). Amplification of MET was observed in up to 20% of NSCLC specimens that had developed acquired resistance to EGFR-TKI (29). Other mechanisms of resistance that are operative in the remaining 30% to 40% of tumors with acquired resistance to EGFR-TKI are under active investigation. EMT has also been associated with acquired resistance to EGFR-TKI (10–12). Recent studies revealed that overexpression of *AXL* led to resistance to EGFR-TKI in NSCLC cells undergoing EMT, and that *AXL* was a potential therapeutic target in patients with acquired resistance to EGFR-TKIs (30, 31). Our present study also showed that the TGF-β1–induced EMT phenomenon encompassed drug insensitivity to gefitinib in A549 cells with wild-type *EGFR* genes.

Several miRNAs have been identified as regulators of EMT. miR-200 family members have been described as main suppressors of EMT by targeting of ZEB1 and ZEB2 (18, 19, 32). In breast cancer, antagonists of miR-21 reversed EMT through targeting PTEN, inactivating AKT and ERK1/2 pathways (33). Our previous study showed that miR-23a regulated TGF-β1–induced EMT by targeting E-cadherin, which encompassed resistance to gefitinib treatment in A549 cells (34). However, the contribution of these miRNAs to resistance to EGFR-TKI was still unclear. In this study, we demonstrated that activation of miR-134 and miR-487b modulated the EMT status and drug resistance to gefitinib through directly targeting *MAGI2*. Correlation between the 14q32 chromosome miRNA cluster and TGF-β–induced EMT has not been reported in human cancer. A recent study showed that overexpression of miR-134 in A549 cells led to promotion of cell proliferation, inhibition of cell apoptosis, and degradation of migration ability (35). Similar alterations of miR-487b and miR-655 have not been found to affect EMT. Previous studies demonstrated that genomic aberrancies located at 14q32 were observed in patients

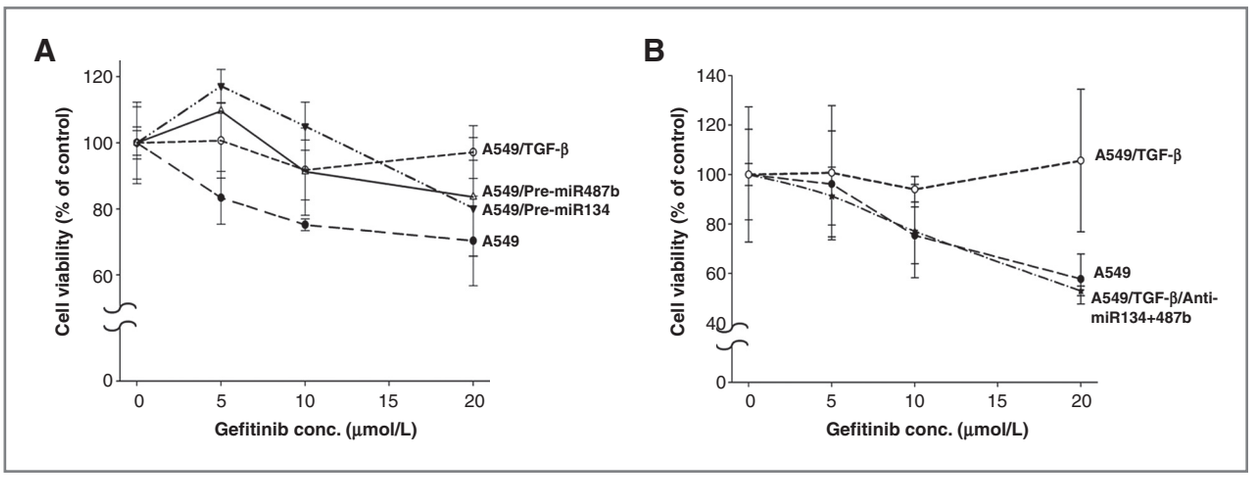

Figure 5. miR-134 and miR-487b mediated drug resistance to gefitinib. A, A549 cells treated with pre-miR-134 or pre-miR-487b for 24 hours were further incubated with various concentrations of gefitinib for 72 hours. B, A549 cells exposed to 5 ng/mL TGF-β1 for 24 hours followed by anti-miR-134 and anti-miR-487b were treated with various concentrations of gefitinib for 72 hours. Each result is expressed as cell viability in the treated samples compared with the untreated sample (100%) for gefitinib therapy. Data, mean ± SD from three independent experiments.

with NSCLC, however, no relationship between 14q32 miRNA cluster alterations and response to EGFR-TKI has been reported (36, 37).

Our present study highlighted a scaffold protein MAGI2, which has nine domains that are potential protein–protein interaction modules, including six PDZ domains, two WW domains, and a guanylate kinase-like domain (38). Expression of MAGI2, which belongs to a membrane-associated guanylate kinase (MAGUK) superfamily, is high in brain and low in other tissues (39). A recent study revealed that *MAGI2* gene rearrangements were implicated in prostate tumorigenesis (40). Inhibition of MAGI2 led to cell migration and proliferation of human hepatocarcinoma cells (27). In our experiments, expression of MAGI2, diminished by TGF-β1, pre-miR-134, and pre-miR-487b treatments, was associated with the EMT phenomenon and acquired resistance to EGFR-TKI. Binding of PTEN to the PDZ domain of MAGI2 enhanced PTEN protein stability and the activity of the downregulating PI3K/Akt signaling cascade (41, 42). Previous studies demonstrated that degradation or loss of PTEN caused PI3K/Akt activation, elicited cell migration and proliferation, and induced the EMT phenomenon (27, 43–45). Absence of PTEN-MAGI2 binding induced PTEN phosphorylation and affected PTEN stability (41, 46). Loss or reduction of PTEN has been associated with acquired EGFR-TKI resistance in our *in vitro* study (47). We confirmed that TGF-β1 stimulation or silencing of MAGI2 led to PTEN phosphorylation and promotion of EMT in A549 cells. MAGI2 may also be associated with EMT by targeting other binding proteins. Previous reports showed that overexpressed MAGI2 interacted with Smad3, a TGF-β downstream molecule, and suppressed Smad3-induced transcriptional activity (48), which mediated TGF-β signaling and regulated many cellular processes (49). An inverse correlation between MAGI2 and Smad3 was reported in tumor samples (50). Taken together, our findings demonstrated that suppression of MAGI2 by the miR-134/487/655 cluster reduced PTEN activity and played an important role in the TGF-β–induced EMT phenomenon.

One limitation of our study is that we were unable to do functional experiments *in vivo* or on clinical samples. To detect EMT *in vivo*, we should view epithelial cells transitioning into fibroblasts and migrating to the interstitium in real time. Unfortunately, this is difficult with current technology. Further studies will be performed using clinical samples to clarify the association between miR-134/487/655 expression and the response to EGFR-TKI in lung adenocarcinoma.

In conclusion, the miR-134/miR-487b/miR-655 cluster promoted the TGF-β1–induced EMT phenomenon and induced resistance to EGFR-TKI in the EMT process by directly targeting *MAGI2*, in which suppression encompassed loss of PTEN stability. A link between MAGI2 and the miRNA cluster was identified as one of the EMT-inducing mechanisms and as a mechanism for development of acquired resistance to EGFR-TKI in lung adenocarcinoma cells without EGFR mutant genes. Our data consequently implied that this link could be a new therapeutic target in patients with advanced lung adenocarcinoma cells undergoing EMT. Further studies should be undertaken to clarify the mechanism of the connection between the miR-134, miR-487b, and miR-655 cluster and EMT in lung adenocarcinoma.

Disclosure of Potential Conflicts of Interest

Kaoru Kubota has honoraria from speakers' bureau from AstraZeneca. No potential conflicts of interest were disclosed by the other authors.

Authors' Contributions

Conception and design: K. Kitamura, M. Seike, T. Okano, H. Mizutani, A. Gemma
Development of methodology: K. Kitamura, T. Okano, H. Mizutani
Acquisition of data (provided animals, acquired and managed patients, provided facilities, etc.): K. Kitamura, T. Okano, K. Matsuda, A. Miyanaga, R. Noro
Analysis and interpretation of data (e.g., statistical analysis, biostatistics, computational analysis): K. Kitamura, T. Okano, K. Matsuda
Writing, review, and/or revision of the manuscript: K. Kitamura, M. Seike, A. Gemma
Administrative, technical, or material support (i.e., reporting or organizing data, constructing databases): Y. Minegishi, A. Gemma
Study supervision: M. Seike, K. Kubota

Acknowledgments

The authors thank C. Soeno and M. Fujishiro of Nippon Medical School for technical assistance.

Grant Support

This study was supported in part by a grant-in-aid from the Ministry of Education, Culture, Sports, Science, and Technology of Japan (grant no. 24591179 to M. Seike; grant no. 25461172 to A. Gemma), MEXT-Supported Program for the Strategic Research Foundation at Private Universities (to M. Seike and A. Gemma), and Smoking Research Foundation (to A. Gemma).

The costs of publication of this article were defrayed in part by the payment of page charges. This article must therefore be hereby marked *advertisement* in accordance with 18 U.S.C. Section 1734 solely to indicate this fact.

Received June 10, 2013; revised October 29, 2013; accepted November 11, 2013; published OnlineFirst November 20, 2013.

References

1. Jemal A, Bray F, Center MM, Ferlay J, Ward E, Forman D. Global cancer statistics. CA Cancer J Clin 2011;61:69–90.
2. Lynch TJ, Bell DW, Sordella R, Gurubhagavatula S, Okimoto RA, Brannigan BW, et al. Activating mutations in the epidermal growth factor receptor underlying responsiveness of non-small-cell lung cancer to gefitinib. N Engl J Med 2004;350:2129–39.
3. Paez JG, Jänne PA, Lee JC, Tracy S, Greulich H, Gabriel S, et al. EGFR mutations in lung cancer: correlation with clinical response to gefitinib therapy. Science 2004;304:1497–500.
4. Mok TS, Wu YL, Thongprasert S, Yang CH, Chu DT, Saijo N, et al. Gefitinib or carboplatin-paclitaxel in pulmonary adenocarcinoma. N Engl J Med 2009;361:947–57.

5. Maemondo M, Inoue A, Kobayashi K, Sugawara S, Oizumi S, Isobe H, et al. Gefitinib or chemotherapy for non-small-cell lung cancer with mutated EGFR. N Engl J Med 2010;362:2380–8.
6. Mitsudomi T, Morita S, Yatabe Y, Negoro S, Okamoto I, Tsurutani J, et al. Gefitinib versus cisplatin plus docetaxel in patients with non-small-cell lung cancer harbouring mutations of the epidermal growth factor receptor (WJTOG3405): an open label, randomised phase 3 trial. Lancet Oncol 2010;11:121–8.
7. Thiery JP, Sleeman JP. Complex networks orchestrate epithelial-mesenchymal transitions. Nat Rev Mol Cell Bio 2006;7:131–42.
8. Thiery JP. Epithelial-mesenchymal transitions in tumour progression. Nat Rev Cancer 2002;2:442–54.
9. Singh A, Greninger P, Rhodes D, Koopman L, Violette S, Bardeesy N, et al. A gene expression signature associated with 'K-Ras addiction' reveals regulators of EMT and tumor cell survival. Cancer Cell 2009; 15:489–500.
10. Yauch RL, Januario T, Eberhard DA, Cavet G, Zhu W, Fu L, et al. Epithelial versus mesenchymal phenotype determines in vitro sensitivity and predicts clinical activity of erlotinib in lung cancer patients. Clin Cancer Res 2005;11:8686–98.
11. Thomson S, Buck E, Petti F, Griffin G, Brown E, Ramnarine N, et al. Epithelial to mesenchymal transition is a determinant of sensitivity of non–small-cell lung carcinoma cell lines and xenografts to epidermal growth factor receptor inhibition. Cancer Res 2005;65:9455–62.
12. Rho JK, Choi YJ, Lee JK, Ryoo BY, Na II, Yang SH, et al. Epithelial to mesenchymal transition derived from repeated exposure to gefitinib determines the sensitivity to EGFR inhibitors in A549, a non-small cell lung cancer cell line. Lung Cancer 2009;63:219–6.
13. Johnson SM, Grosshans H, Shingara J, Byrom M, Jarvis R, Cheng A, et al. Ras is regulated by the let-7 microRNA family. Cell 2005; 120:635–647.
14. Lu J, Getz G, Miska EA, Alvarez-Saavedra E, Lamb J, Peck D, et al. MicroRNA expression profiles classify human cancers. Nature 2005; 435:834–8.
15. Volinia S, Calin GA, Liu CG, Ambs S, Cimmino A, Petrocca F, et al. A microRNA expression signature of human solid tumors defines cancer gene targets. Proc Natl Acad Sci USA 2006;103:2257–61.
16. Yanaihara N, Caplen N, Bowman E, Seike M, Kumamoto K, Yi M, et al. Unique microRNA molecular profiles in lung cancer diagnosis and prognosis. Cancer Cell 2006;9:189–98.
17. Seike M, Goto A, Okano T, Bowman ED, Schetter AJ, Horikawa I, et al. MiR-21is an EGFR-regulated anti-apoptonic factor in lung cancer in never-smokers. Proc Natl Acad Sci U S A 2009;106:12085–90.
18. Ceppi P, Mudduluru G, Kumarswamy R, Rapa I, Scagliotti GV, Papotti M, et al. Loss of miR-200c expression induces an aggressive, invasive, and chemoresistant phenotype in non-small cell lung cancer. Mol Cancer Res 2010;8:1207–16.
19. Gregory PA, Bert AG, Paterson EL, Barry SC, Tsykin A, Farshid G, et al. The miR-200 family and miR-205 regulate epithelial to mesenchymal transition by targeting ZEB1 and SIP1. Nat Cell Biol 2008;10:593–601.
20. Gemma A, Takenaka K, Hosoya Y, Matuda K, Seike M, Kurimoto F, et al. Altered expression of several genes in highly metastatic subpopulations of a human pulmonary adenocarcinoma cell line. Eur J Cancer 2001;37:1554–61.
21. Seike M, Yanaihara N, Bowman ED, Zanetti KA, Budhu A, Kumamoto K, et al. Use of a cytokine gene expression signature in lung adenocarcinoma and the surrounding tissue as a prognostic classifier. J Natl Cancer Inst 2007;99:1257–69.
22. Gemma A, Li C, Sugiyama Y, Matsuda K, Seike Y, Kosaihira S, et al. Anticancer drug clustering in lung cancer based on gene expression profiles and sensitivity database. BMC Cancer 2006;6:174.
23. Miyanaga A, Gemma A, Noro R, Kataoka K, Matsuda K, Nara M, et al. Antitumor activity of histone deacetylase inhibitors in non-small cell lung cancer cells: development of a molecular predictive model. Mol Cancer Ther 2008;7:1923–30.
24. Shimokawa T, Seike M, Soeno C, Uesaka H, Miyanaga A, Mizutani H, et al. Enzastaurin has anti-tumour effects in lung cancers with over-expressed JAK pathway molecules. Br J Cancer 2012;106:867–75.
25. Mizutani H, Okano T, Minegishi Y, Matsuda K, Sudoh J, Kitamura K, et al. HSP27 modulates epithelial to mesenchymal transition of lung cancer cells in a Smad-independent manner. Oncol Lett 2010;1: 1011–6.
26. Mimae T, Okada M, Hagiyama M, Miyata Y, Tsutani Y, Inoue T, et al. Upregulation of notch2 and six1 is associated with progression of early-stage lung adenocarcinoma and a more aggressive phenotype at advanced stages. Clin Cancer Res 2012;18:945–55.
27. Hu Y, Li Z, Guo L, Wang L, Zhang L, Cai X, et al. MAGI-2 inhibits cell migration and proliferation via PTEN in human hepatocarcinoma cells. Arch Biochem Biophys 2007;467:1–9.
28. Kobayashi S, Boggon TJ, Dayaram T, Jänne PA, Kocher O, Meyerson M, et al. EGFR mutation and resistance of non-small-cell lung cancer to gefitinib. N Engl J Med 2005;352:786–92.
29. Engelman JA, Zejnullahu K, Mitsudomi T, Song Y, Hyland C, Park JO, et al. MET amplification leads to gefitinib resistance in lung cancer by activating ERBB3 signaling. Science 2007;316:1039–43.
30. Byers LA, Diao L, Wang J, Saintigny P, Girard L, Peyton M, et al. An epithelial-mesenchymal transition gene signature predicts resistance to EGFR and PI3K inhibitors and identifies Axl as a therapeutic target for overcoming EGFR inhibitor resistance. Clin Cancer Res 2013;19: 279–90.
31. Zhang Z, Lee JC, Lin L, Olivas V, Au V, LaFramboise T, et al. Activation of the AXL kinase causes resistance to EGFR-targeted therapy in lung cancer. Nat Genet 2012;44:852–60.
32. Bracken CP, Gregory PA, Kolesnikoff N, Bert AG, Wang J, Shannon MF, et al. A double-negative feedback loop between ZEB1-SIP1 and the microRNA-200 family regulates epithelial-mesenchymal transition. Cancer Res 2008;68:7846–54
33. Han M, Liu M, Wang Y, Chen X, Xu J, Sun Y, et al. Antagonism of miR-21 reserves Epithelial-mesenchymal transition and cancer stem cell phenotype through AKT/ERK1/2 inactivation by targeting PTEN. PLoS One 2012;7:e39520
34. Cao M, Seike M, Soeno C, Mizutani H, Kitamura K, Minegishi Y, et al. MiR-23a regulates TGF-β-induced epithelial-mesenchymal transition by targeting E-cadherin in lung cancer cells. Int J Oncol 2012;41:869–75.
35. Zhang X, Wang H, Zhang S, Song J, Zhang Y, Wei X, et al. MiR-134 functions as a regulator of cell proliferation, apoptosis, and migration involving lung septation. In Vitro Cell Dev Biol Anim 2012;48: 131–6.
36. Gallegos Ruiz MI, Floor K, Roepman P, Rodriguez JA, Meijer GA, Mooi WJ, et al. Integration of gene dosage and gene expression in non-small cell lung cancer, identification of HSP90 as potential target. PLoS One 2008;3:e0001722.
37. Choi JS, Zheng LT, Ha E, Lim YJ, Kim YH, Wang YP, et al. Comparative genomic hybridization array analysis and real-time PCR reveals genomic copy number alteration for lung adenocarcinomas. Lung 2006; 184:355–62.
38. Xu J, Paquet M, Lau AG, Wood JD, Ross CA, Hall RA. β1-adrenergic receptor association with the synaptic scaffolding protein membrane-associated guanylate kinase inverted-2 (MAGI-2). Differential regulation of receptor internalization by MAGI-2 and PSD-95. J Biol Chem 2001;276:41310–7.
39. Hirao K, Hata Y, Ide N, Takeuchi M, Irie M, Yao I, et al. A novel multiple PDZ domain-containing molecule interacting with N-methyl-D-aspartate receptors and neuronal cell adhesion proteins. J Biol Chem 1998;273:21105–10
40. Berger MF, Lawrence MS, Demichelis F, Drier Y, Cibulskis K, Sivachenko AY, et al. The genomic complexity of primary human prostate cancer. Nature 2011;470:214–20.
41. Tolkacheva T, Boddapati M, Sanfiz A, Tsuchida K, Kimmelman AC, Chan AM. Regulation of PTEN binding to MAGI-2 by two putative phosphorylation sites at threonine 382 and 383. Cancer Res 2001; 61:4985–9.
42. Valiente M, Andrés-Pons A, Gomar B, Torres J, Gil A, Tapparel C, et al. Binding of PTEN to specific PDZ domains contributes to PTEN protein stability and phosphorylation by microtubule-associated serine/threonine kinases. J Biol Chem 2005;280:28936–43.
43. Bowen KA, Doan HQ, Zhou BP, Wang Q, Zhou Y, Rychahou PG, et al. PTEN loss induces epithelial–mesenchymal transition in human colon cancer cells. Anticancer Res 2009;29:4439–49.

44. Wang H, Quah SY, Dong JM, Manser E, Tang JP, Zeng Q. PRL-3 down-regulates PTEN expression and signals through PI3K to promote epithelial-mesenchymal transition. Cancer Res 2007;67:2922–6.
45. Mulholland DJ, Kobayashi N, Ruscetti M, Zhi A, Tran LM, Huang J, et al. Pten loss and RAS/MAPK activation cooperate to promote EMT and metastasis initiated from prostate cancer stem/progenitor cells. Cancer Res 2012;72:1878–89.
46. Vazquez F, Ramaswamy S, Nakamura N, Sellers WR. Phosphorylation of the PTEN tail regulates protein stability and function. Mol Cell Biol 2000;20:5010–8.
47. Kokubo Y, Gemma A, Noro R, Seike M, Kataoka K, Matsuda K, et al. Reduction of PTEN protein and loss of epidermal growth factor receptor gene mutation in lung cancer with natural resistance to gefitinib (IRESSA). Br J Cancer 2005;92:1711–9.
48. Shoji H, Tsuchida K, Kishi H, Yamakawa N, Matsuzaki T, Liu Z, et al. Identification and characterization of a PDZ protein that interacts with activin type II receptors. J Biol Chem 2000;275: 5485–92.
49. Ross KR, Corey DA, Dunn JM, Kelley TJ. SMAD3 expression is regulated by mitogen-activated protein kinase kinase-1 in epithelial and smooth muscle cells. Cell Signal 2007;19:923–31.
50. Han B, Chen XW, Wang X, Michaelis EK. Integrating multiple microarray data for cancer pathway analysis using bootstrapping K-S test. J Biomed Biotechnol 2009;2009:707580.